Available online at www.sciencedirect.com
ScienceDirect
Applied Surface Science 253 (2007) 7260–7264
applied surface science
www.elsevier.com/locate/apsusc

# Protective hybrid sol–gel coatings containing bioactive particles on surgical grade stainless steel: Surface characterization

Josefina Ballarre [a,*], Damián A. López [a], Wido H. Schreiner [b], Alicia Durán [c], Silvia M. Ceré [a]

[a] *INTEMA, Universidad Nacional del Mar del Plata, Juan B. Justo 4302, B7608FDQ Mar del Plata, Argentina*
[b] *LSI-LANSEN, Departamento de Física, UFPR, CP 19081, 81531-990 Curitiba, Brazil*
[c] *Instituto de Cerámica y Vidrio (CSIC), Campus de Cantoblanco, 28049 Madrid, Spain*

Received 22 January 2007; received in revised form 2 March 2007; accepted 3 March 2007
Available online 12 March 2007

**Abstract**

Metallic materials are the most used materials as orthopaedic or dental implants for their excellent mechanical properties. However, they are not able to create a natural bonding with the mineralized bone and they could release metallic particles that could finally end in the removal of the implant. One way to avoid these effects is to protect the metallic implant with a biocompatible coating. In this work there are analyzed two kinds of protective organic–inorganic sol–gel made coatings with the adding of glass-ceramic particles with the aim of generating bioactivity. The samples are surface characterized by SEM, XRD and XPS. Amorphous hydroxyapatite (aHAp) deposited on the samples after 30 days of immersion in simulated body fluid (SBF) is detected on the samples and its presence is considered as a first signal of bioactivity.


*Keywords:* Stainless steel; Coatings; Surface characterization; Bioactivity

## 1. Introduction

When a surgeon has to choose a material for a permanent implant, orthopaedic or dental, specific mechanical properties for each case are required. It is also important to analyze the toxicity or reactions of the implant with surrounding tissue. Metals are the most commonly used materials that fulfil the requirements of low toxicity and good mechanical properties [1]. However, metals do not develop a chemical bond with bone and wear and corrosion of the metallic implant overtime can lead to the release of metallic particles causing different pathologies that could finally end in the removal of the implant [2,3]. Among the standard surgical implant materials, the most used are stainless steel 316L (ASTM F138), Co based alloys (mainly ASTM F75, and F799) and titanium alloys, where Ti–6Al–4V (ASTM F67 and F136) are the most used. AISI 316L stainless steel is widely used in applications where the implant is temporary, although it is also used as permanent implants in developing countries.

One of the ways to improve the ion release form the alloy is to coat the metallic implant with a protective layer, which could be functionalized with the addition of bioactive particles to the films. Therefore, the coating could act as a barrier avoiding the release of metal ions and the particles reaction could make a bonding with the old bone by the formation of hydroxyapatite [4,5]. Many coatings were used to improve the performance of metallic prosthesis, and one that showed biocompatibility was the silica based type with silane precursors. The attainment of these films by sol–gel process has been successfully used on stainless steel, silver and aluminium and has improved the oxidation and corrosion resistance of these metals [6,7]. It is possible to replace some inorganic components for organic ones, giving more plasticity to the structure [8]. The combination of the sol–gel organic–inorganic (hybrid) films with the addition of bioactive particles from the system $SiO_2$–$P_2O_5$–CaO has shown a good adherence of the cement-less implants with the pre-existing bone [9–11].

The objective of this work is to protect AISI 316L stainless steel with a hybrid coating with a high content of organic compounds loaded with glass-ceramic particles (which are

* Corresponding author at: INTEMA, División Corrosión, UNMdP, Av. Juan B. Justo 4302, B7608FDQ Mar del Plata, Argentina. Tel.: +54 223 4816600; fax: +54 223 4810046.
*E-mail address:* jballarre@fi.mdp.edu.ar (J. Ballarre).

0169-4332/$ – see front matter © 2007 Elsevier B.V. All rights reserved.
doi:10.1016/j.apsusc.2007.03.007

potentially able to induce bioactivity on the surface trough the deposition of hydroxyapatite). These coatings could become bioactive, leading to the formation of new bone. Hybrid coatings with high content of organic compounds are synthesized with the aim of providing thick coatings formed by two interpenetrated (organic and inorganic) networks that should enhance the metal protection. The coatings present an outer plastic and open structure to allow the electrolyte access to the particle, and through its reaction induce the formation of hydroxyapatite [12,13] short coming the bioactive response when compared with the previous obtained coatings [14].

## 2. Experimental

### 2.1. Substrates

Flat samples of stainless steel AISI 316L (Altantic Stainless Co. Inc., composition: C 0.03% max, Mn 2% max, Si 1% max, P 0.045% max, S 0.03% max, Ni 10–14%, Cr 16–18%, and Mo 2–3%) of 2 cm × 1 cm area were used as substrates. They were sequentially cleaned with a soap solution, isopropylic alcohol and ultrasound bath before the application of the coating.

### 2.2. Sol–gel sol

Two types of sols were used for the coatings: (1) TEOS (tetraethoxysilane)-MTES (methyltriethoxysilane), (2) TMH (TEOS (tetraethoxysilane)-γMPS (3-methacrylopropyl trimethoxysilane)-HEMA (2-hydroxyethyl methacrylate)). The TEOS-MTES sol was prepared by acid catalysis method in one stage, using TEOS (ABCR), and MTES (ABCR) as silica precursors; absolute ethanol as solvent and 0.1N nitric and acetic acids as catalysts. The water was incorporated from the nitric acid solution in stoichiometric ratio. The molar ratio of TEOS/MTES was 40:60. All the reagents were stirred at 40 °C during 3 h obtaining a transparent sol (pH 1–2, viscosity = 2.6 mPa s). The TEOS (ABCR)-γMPS (Dow Corning)-HEMA (Aldrich) (TMH) sol was made in a two steps procedure using 0.1N nitric acid and isopropylic alcohol. The solution, containing 40 g $l^{-1}$ of $SiO_2$, was stirred at 65 °C for 36 h in glycerine bath.

### 2.3. Glass-ceramic particles

The glass-ceramic particles were made from a precursor glass of the system $SiO_2$–$P_2O_5$–CaO. The precursors used were silica sand, calcium carbonate (Aldrich) and orthophosphoric acid (Aldrich). The ratio of each one was calculated in order to obtain the concentration of CaO of 47.29%, $SiO_2$ 35.69% and $P_2O_5$ 17.01% in weight in the final glass. The mixture was fused in a platinum crucible at 1600 °C in air atmosphere, and then quenched in water. The thermal treatment was made at 1050 °C for 2 h in an electric furnace with the aim of obtaining apatite and wollastonite as crystalline phases. The glass-ceramic obtained was milled in an agate planetary mill (Frizsth Pulverisette, Germany), using a speed of rotation of 1500 rpm for 4 h. After this process, the particles were screened with Tyler screens (nos. 270, 325 and 600) to obtain different diameter size distribution of bioactive particles. Two particle size distributions were used: (a) ''small particles'' (s.p.) for particles with diameter less than 20 μm; and (b) ''big particles'' (b.p.) for particles with diameter bigger than 20 μm but smaller than 45 μm.

### 2.4. Suspensions

The particle suspensions were prepared by the addition of 10% in weight of particles with respect to the solution [15]. The suspensions were stirred by a high shear mixing in a rotor-stator agitator (Silverson L2R, UK) during 6 min. After the first 3 min, 5–20% by weight on solids of Triton X 114 Surfactant (Dow Corning) was added as dispersant in the glass-ceramic containing suspensions. The Triton works as a surfactant that adsorbs on the surface of the glass-ceramic particles, creating an electrostatic repulsion between the particles and avoiding segregation.

### 2.5. Coatings

Coatings were obtained by the dip-coating technique at room temperature, and withdrawn at 25 cm $min^{-1}$. Experimental details shown elsewhere [16,17]. The different types of coatings were used in this work are the following:

(a) A single layer of TEOS-MTES heat treated at 450 °C during 30 min, and then a second layer deposited on top of it consisting in two layers of TMH (without thermal treatment in between).
(b) A single layer of TEOS-MTES treated at 450 °C during 30 min, and then a second layer deposited on top of if consisting in two layers of TMH hybrid (without thermal treatment in between), followed by a third layer of TMH containing a suspension of 10% weigh in volume of bioactive particles (either small or big particles).
(c) Two layers of TMH without thermal treatment in between.
(d) Two layers of TMH without thermal treatment in between followed by a third layer of TMH containing a suspension of 10% weigh in volume of bioactive particles (some samples with small particles and some with big ones).

Finally all types of coatings were heat treated at 150 °C for 60 min in air atmosphere.

The coating thickness were measured on glass samples by using a profilometer (Talystep, Taylor-Hobson, UK) on a scratch made immediately after deposition. The average of three measurements was taking as the final value.

### 2.6. Surface analysis

A simulated body fluid (SBF) solution was used as electrolyte in all the experiments. SBF was prepared with the following chemical composition [18]: NaCl (8.053 g $l^{-1}$), KCl (0.224 g $l^{-1}$), $CaCl_2$ (0.278 g $l^{-1}$), $MgCl_2{\cdot}6H_2O$ (0.305 g $l^{-1}$), $K_2HPO_4$ (0.174 g $l^{-1}$), $NaHCO_3$ (0.353 g $l^{-1}$),

$(CH_2OH)_3CNH_2$ (6.057 g $l^{-1}$). Concentrated hydrochloric acid (HCl) was added to adjust the pH to 7.25 ± 0.05.

The samples were immersed in SBF for 24 h and 30 days, and sealed at 37 °C in a sterilized furnace until the tests were done.

XPS essays of the samples were made with a base pressure in the experimental chamber lower than $10^{-9}$ mbar. The spectra were collected using Mg Kα (1253.6 eV) radiation and the overall energy resolution was about 0.8 eV. Survey spectra were recorded for the samples in the 0–1100 eV kinetic energy range by 1 eV steps. High resolution scans with 0.1 eV steps were conducted over the following regions of interest: Fe 2p, Cr 2p, Ni 2p and Ca 2p. In all the cases surface charging effects were compensated by referencing the binding energy (BE) to the C 1s line of residual carbon set at 284.5 eV BE [19]. Spectral decomposition assumed mixed Gaussian–Lorenzian curves and was performed by using background subtraction and a least square fitting program. The samples were measured after 30 min of $Ar^+$ sputtering performed with an argon ion gun under an accelerating voltage of 3 kV. For the analysis of calcium species the samples were measured before the $Ar^+$ ion sputtering.

XRD tests were made on the samples using Mg Kα (1253.6 eV) radiation, a current of 50 mA, voltage of 40 kV, scan step size of 0.02° and a time per step of 0.5 s.

Scanning electronic microscopy (SEM, Phillips XL 30), X-ray diffraction (XRD, Philips X'Pert MPD) and X-ray photoelectron spectroscopy (XPS, commercial VG ESCA 3000) essays were made with the aim of characterizing surface reactions of the samples after 30 days of immersion in SBF.

Images of the coatings with the two kinds of particles were taken by SEM and segmented with a proposed build algorithm developed in Mathlab® 6.5 [20]. It work with standard functions of this language and a specific library called SDC Morphology Toolbox (SDC, 2001), with functions of Mathematic Morphology. The algorithm used a growth of regions method, known as Watershed Transformed. The markers for this Transformed are determined with a patron classification method. Starting from the binary image obtained by segmentation the particle density (area occupied by the particles/total sample area) was determined over the films after 30 days of immersion in SBF.

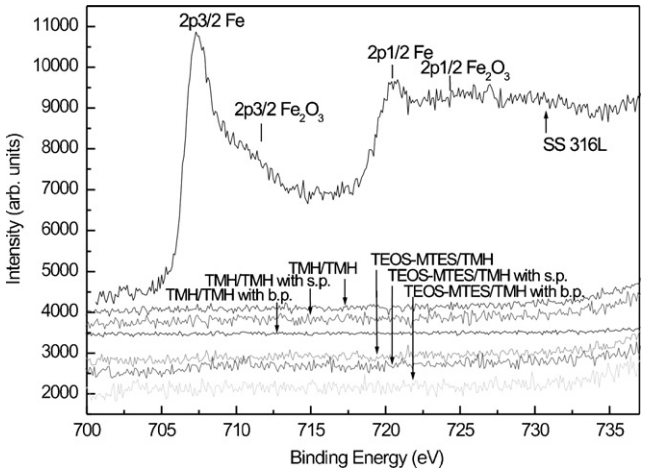


Fig. 1. XPS spectra for Fe 2p region with 30 s of sputtering with $Ar^+$ for the stainless steel 316L, and all the coated systems under study after being immersed for 30 days in SBF.

## 3. Results and discussion

Homogeneous and crack-free coatings (when observed with optic microscopy up to 500×) were obtained on stainless steel 316L. The average thickness measured for the TMH/TMH film without and with small and big particles were 3.5, 6.8 and 5.9 μm, respectively. The thickness for the TEOS-MTES/TMH film without particles was 1.8 μm and the values for the samples with small and big particles were 7.8 and 8.4 μm, respectively.

Fig. 1 presents the high resolution XPS scans for Fe 2p region after 30 min sputtering with $Ar^+$ ions for all samples under study after 30 days of immersion in SBF. The TEOS-MTES/TMH and TMH/TMH samples immersed for 30 days in

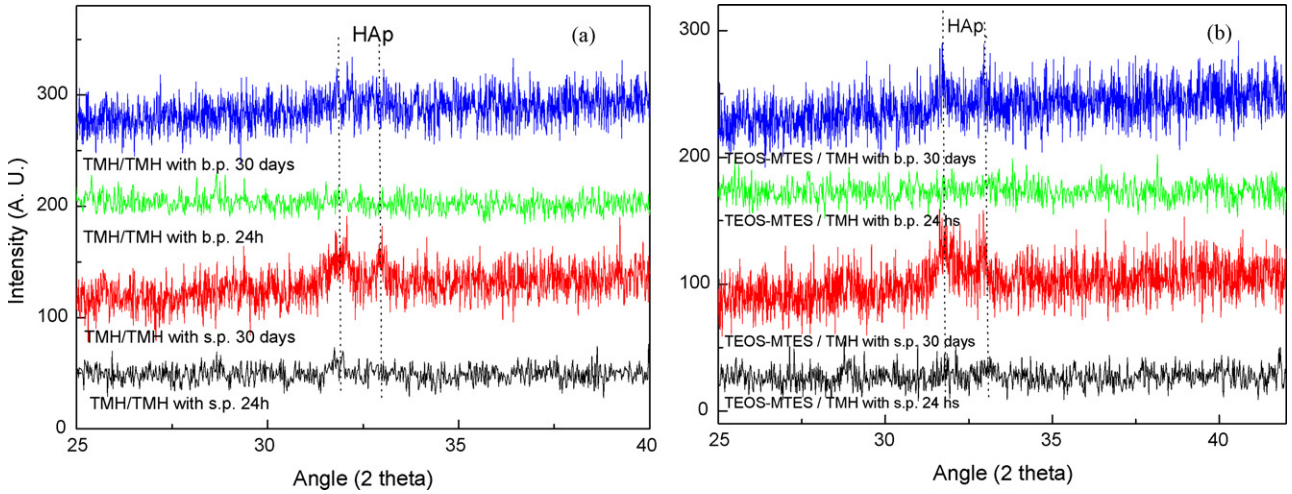


Fig. 2. XRD spectra showing the HAp zone for (a) the TMH/TMH coating with small and big particles after 24 h and 30 days of immersion in SBF and (b) the TEOS-MTES/TMH coating with small and big particles after 24 h and 30 days of immersion in SBF.

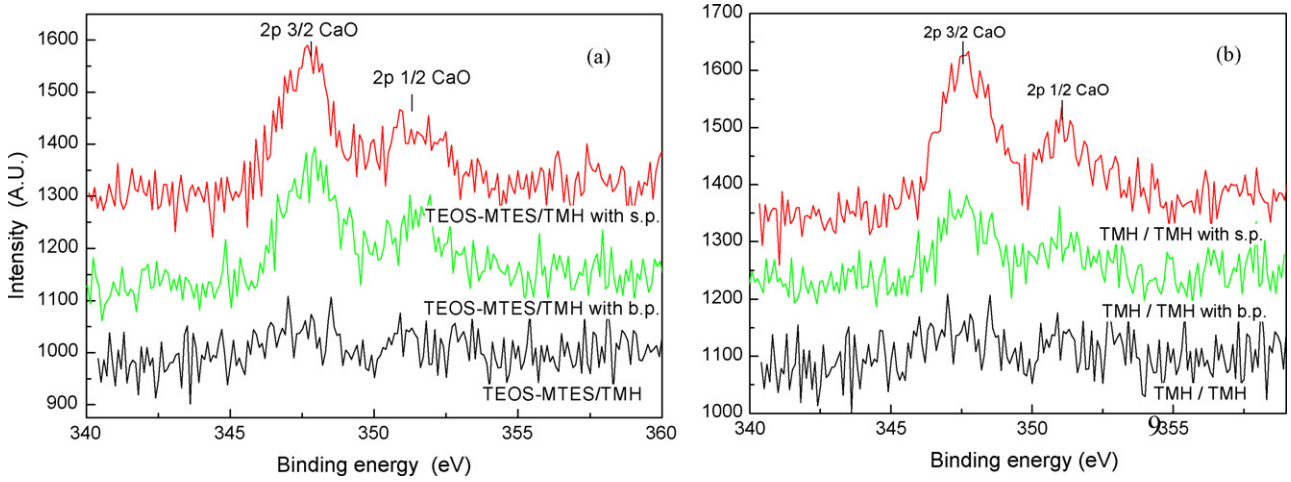


Fig. 3. XPS spectra for Ca 2p region without sputtering with $Ar^+$ for (a) TEOS-MTES/TMH coating without and with the two sizes of particles and (b) TMH/TMH coating without and with the two sizes of particles, immersed for 30 days in SBF.

SBF did not present Fe ions neither in the coatings without particles nor in the samples with the two sizes of particles for both coating system. The same kind of results were found in the Ni 2p and Cr 2p regions after 30 min of sputtering (not shown). Only the samples without any coating (bare stainless steel) presented the characteristic peaks of the Cr, Fe and Ni oxides. These results show that the metallic ions of the substrate did not migrate across the coating after 30 days of immersion in SBF.

Fig. 2 shows the X-ray diffraction (XRD) pattern obtained for the samples containing particles. The samples with TMH/TMH coating containing either small or big particles after 24 h and 30 days of immersion in SBF are shown in Fig. 2(a), while samples with TEOS-MTES/TMH coatings containing either small or big particles are shown in Fig. 2(b). Both figures show the presence of amorphous hydroxyapatite (aHAp) with peaks at 31.8° and 32.9° corresponding to the calcium hydroxide phosphate ICSD # 026205 [21]. Those two peaks appear when it is analyzed the deposition of aHAp after 30 days of immersion in SBF by XRD and there is no evidence of them in the samples with 24 h of immersion in SBF.

In Fig. 3(a) and (b) the spectra of the TMH/TMH and TEOS-MTES/TMH coated samples without particles, and with small or big particles are respectively shown. The scans were made after 30 days of immersion in SBF and the XPS assays were conducted without any sputtering with $Ar^+$ ions. No depth profiling was done because the deposition of the hydroxyapatite is only superficial. It can be observed the presence of two peaks in the Ca region in both figures. The peaks are associated with the 2p Ca 3/2 (347.5 eV) and 2p Ca 1/2 (351 eV) of the HAp [22,23]. The signal is present in the samples with both kinds of particles, showing stronger intensities in the samples containing small particles. These data are in good agreement with those of XRD presented above.

Figs. 4 and 5 show photomicrographs of the surface films with TEOS-MTES/TMH coating with the same magnification (100×) after 24 h and 30 days of immersion in SBF, with the two sizes of particles. It can be observed the deposition of a few atomic layers of aHAp after 30 days of immersion in the samples containing small particles (Fig. 4(b)), presenting a higher proportion of aHAp deposition than the samples with big particles (see Fig. 5(b)). The same kind of results is observed for TMH/TMH coatings (not shown). The analysis of these results by the Watershed Transformed essays, show a aHAp density of 53.9% and 57.5% for the samples with TMH/TMH and TEOS-MTES/TMH coatings with small particles, and a particle density of 39.5 and 32.7% for the same coated samples with big particles after 30 days of immersion in SBF (not shown).

In vitro tests revealed that all the coating containing particles induced the formation of aHAp as a result of the chemical

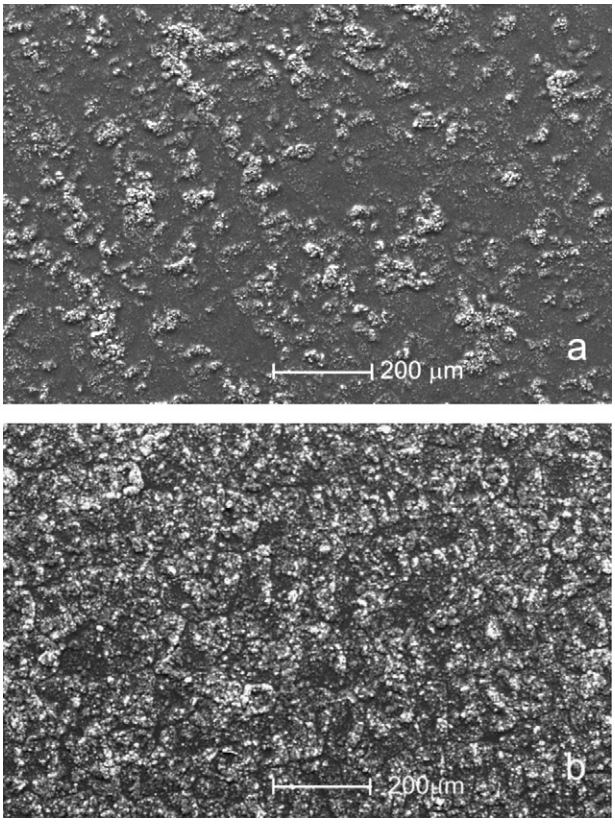


Fig. 4. Surface morphology of TEOS-MTES/TMH coating on stainless steel 316L with small particles, after (a) 24 h and (b) 30 days of immersion in SBF.

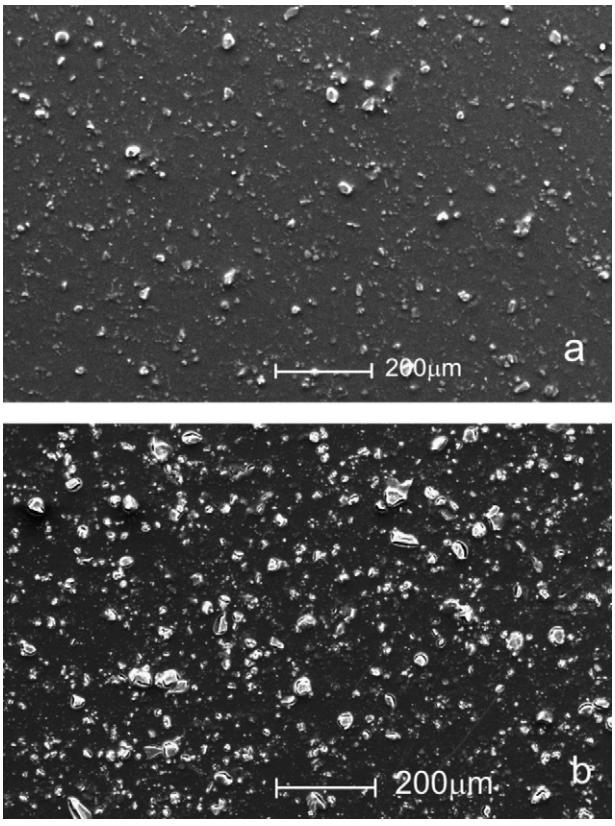


Fig. 5. Surface morphology of TEOS-MTES/TMH coating on stainless steel 316L with big particles, after (a) 24 h and (b) 30 days of immersion in SBF.

reaction of the particles with the SBF. The deposition of semi-crystalline HAp is considered as a first signal of bioactivity [24,25]. As the coatings containing small particles present a higher reactive area, it is not surprising that they are able to induce a higher proportion of aHAp deposition on the surface, than the coating with big particles. Therefore, smaller particles could be considered to have a better bioactive response than bigger ones.

However, it is important to consider another aspect related to these coatings that is the protective function. It has been already studied that the particle reaction to form aHAp breaks the coating that contains the particles inducing cracks in the surrounding of the particle [26,27]. This fact could lead to localized corrosion of the substrate if the flaws reach the substrate; not being tolerated in an implant in service due to the entrance of electrolyte in the cracks formed on the coating. The TMH coating, containing a high proportion of organic compounds should improve the performance of the coating diminishing crack propagation when compared with the more inorganic ones [27] maintaining or even enhancing the bioactive response of the coatings with the new proposed formulation.

It is also important to note that the inner layer of TEOS-MTES or TMH applied to the AISI 316L substrates, does not affect the bioactive response of the samples. The more inorganic coating should provide a protective barrier enhancing the corrosion resistance of the substrate when compared with the more organic system. Electrochemical experiments are being conducted to get a better insight on this field with the objective to select the best coating for the system under study.

## 4. Conclusions

The TEOS-MTES/TMH and TMH/TMH samples immersed for 30 days in SBF did not present Fe ions neither on their surface nor on the samples with the two sizes of particles for both coating system. These results show that the metallic ions of the substrate did not migrate across the coating.

XRD and XPS essays evidence the presence of aHAp after 30 days of immersion in SBF, while the samples with 24 h did not present this deposition.

## Acknowledgements

The authors wish to thank to SeCyT – CAPES Cooperation Project (078/04) and PICTO 11338 (ANCyT-UNMdP). The participation of Eng. Mariela Azul Gonzalez (UNMdP) is gratefully acknowledged.

## References

[1] K.S. Katti, Colloids Surf. B: Biointerf. 39 (2004) 133.
[2] Y. Okazaki, E. Goloh, T. Manabe, K. Kobayashi, Biomaterials 25 (2004) 5913.
[3] J. Woodman, J. Black, D. Nunamaker, J. Biomed. Mater. Res. 17 (1983) 655.
[4] L. Guan, R. Pilliar, Biomaterials 25 (2004) 5303.
[5] L. Guan, J. Wang, A. Tache, N. Valiquette, D. Deporter, R. Pilliar, Biomaterials 25 (2004) 5313.
[6] O. de Sanctis, L. Gomez, N. Pellegri, C. Parodi, A. Marajofsky, A. Durán, J. Non-Cryst. Solids 121 (1990) 338.
[7] O. de Sanctis, L. Gomez, N. Pellegri, A. Durán, Surf. Coat. Technol. 70 (1995) 251.
[8] L.E. Amato, D.A. López, P.G. Galliano, S.M. Ceré, Mater. Lett. 59 (2005) 2006.
[9] J. Williams, L. Reister, in: Proceedings of the 20th Annual Meeting of the Society for Biomaterials, vol. 17, 1994, p. 179.
[10] J. Ballarre, J.C. Orellano, C. Bordenave, P.G. Galliano, S.M. Ceré, J. Non-Cryst. Solids 304 (2002) 278.
[11] O. Peitl, E.D. Zanotto, L.L. Hench, J. Non-Cryst. Solids 292 (2001) 115.
[12] T. Kokubo, Acta Mater. 46 (7) (1998) 2519–2527.
[13] T. Kokubo, H. Takadama, Biomaterials 27 (2006) 2907–2915.
[14] P.G. Galliano, J.J. de Damborenea, M.J. Pascual, A. Durán, J. Sol–Gel Sci. Technol. 13 (1998) 723.
[15] C. García, A. Durán, R. Moreno, J. Sol–Gel Sci. Technol. 34 (2005) 1–7.
[16] P.C. Innocenzi, M. Guglielmi, M. Gobbin, P. Colombo, J. Eur. Ceram. Soc. 10 (1992) 431–436.
[17] M. Guglielmi, S. Zenezini, J. Non-Cryst. Solids 121 (1990) 303–309.
[18] T. Kokubo, H. Kushitani, S. Sakka, T. Kitsugi, T. Yamamuro, J. Biomed. Mater. Res. 24 (1990) 721.
[19] J.F. Moulder, W.F. Stickle, P.E. Sobol, K.D. Bomben (Eds.), Handbook of X-Ray Photoelectron Spectroscopy, Physical Electronics, Inc., Eden Praire, MN, USA, 1995.
[20] González M.A., Ballarín V., Announcement of the 35th Informatic and Operative Research Meeting, JAIIO-SIS, (2006) 11.
[21] K. Sudarsanan, R.A. Young, Acta Crystallogr. B 25 (1969) 1534.3.
[22] L.A. de Sena, N.C.C. Rocha, M.C. Andrade, G.A. Soares, Surf. Coat. Technol. 166 (2003) 254.
[23] M. Hsieh, L. Perng, T. Chin, Mater. Chem. Phys. 74 (2002) 245.
[24] C. Ohtsuki, T. Kokubo, T. Yamamuro, J. Non-Cryst. Solids 143 (1992) 84.
[25] X. Liu, C. Ding, P. Chu, Biomaterials 25 (2004) 1755.
[26] C. García, S. Ceré, A. Durán, J. Non-Cryst. Solids 348 (15) (2004) 218.
[27] C. García, S. Ceré, A. Durán, J. Non-Cryst. Solids 352 (32–35) (2006) 3488.